Water Immobilization at Surfactant Interfaces in Reverse Micelles

Ruth E. Riter, Dale M. Willard, and Nancy E. Levinger*

Department of Chemistry, Colorado State University, Fort Collins, Colorado 80523-1872

Received: October 14, 1997; In Final Form: January 16, 1998

The mobility of water in water/Aerosol OT (AOT)/isooctane reverse micelles has been investigated via polar solvation dynamics measurements using ultrafast, time-resolved fluorescence-upconversion spectroscopy. For the smallest reverse micelles studied, $w_0 = 1.1$, no solvation dynamics are observed on the time scale of the instrument, suggesting that the water is essentially frozen. As w_0 increases, the mobility of water increases, and the time-correlation functions exhibit multiexponential decays. A subpicosecond component is observed on a time scale similar to that of diffusive bulk-water motion.[1] The other components decay on time scales of a few picoseconds to hundreds of picoseconds. The amplitude of the solvent response increases as w_0 increases, which is attributed to increased mobility of the water inside the reverse micelles. Because the micellar interior is highly ionic, the solvation dynamics of coumarin 343 in a 1 M Na^+ (Na_2SO_4) solution were also investigated to compare the dynamics of water in the reverse micelles with the dynamics of bulk water in an ionic solution.

Introduction

Restrictive environments are known to favorably facilitate many chemical and physical processes. The efficiency of biological reactions, such as electron and proton transfer, is attributed, in part, to the highly structured environments in which they take place.[2,3] Catalytic and separation processes are enhanced by employing gels, micelles, polymers, zeolites, clays, and biological membranes.[4−6] To investigate the effects of structured environments on chemical dynamics, it is advantageous to choose simple models with well-characterized physical and chemical attributes.

Micellar solutions are model systems that have been used extensively to investigate restricted environments.[7,8] Micelles are multicomponent systems where a given solvent is isolated from a continuous-phase solvent by a surfactant or surfactant and cosurfactant pair. Reverse micelles are composed of a polar solvent sequestered by a surfactant in a nonpolar solvent. For reverse micelles, the interaction of the surfactant polar headgroups with the polar solvent can result in the formation of a well-defined solvent pool. These isolated solvent pools can be thought of as nanobeakers where reactions take place as the micelles exchange reactants.[9] Not only is the reactant concentration controllable by the micelles,[10] reactivity is often enhanced by the micellar structure and unique nanoenvironment.[7,8,11−13]

One common surfactant used to form reverse micelles is Aerosol-OT (AOT).[14] AOT reverse microemulsions exhibit a wide range of structures including discrete water droplets, interconnected bicontinuous water channels, and interacting rods. The most widely investigated structure that has been probed is the monodisperse spherical water droplets, reverse micelles. The droplet sizes are directly related to the water volume-to-surfactant surface-area ratio defined as the molar ratio of water to AOT:

$$w_0 = \frac{[H_2O]}{[AOT]} \tag{1}$$

AOT is an anionic surfactant complexed to a counterion, typically sodium. The water molecules in the intramicellar water pool are either free or bound to the interface.[15−33] The bound water can interact with various components of the surfactant. These interactions include hydrogen-bonding interactions with oxygen molecules on the sulfonate and succinate groups, ion−dipole interactions with the anionic surfactant headgroup and counterion, dipole−dipole interactions with the succinate group, and dispersive forces with the hydrocarbon tails.

Many characteristics of AOT reverse micelles have been investigated.[14] Using static spectroscopic studies, Wong et al.[17,18] reported that as the micellar radius increased, the polarity of the water pool increased. They attribute the increased polarity to an increase in the number of free water molecules in the water pool and suggest that Na^+/water interactions cause a rigid water structure in reverse micelles with $w_0 = 1.5$. Belletête et al.[23] observed that the effective dielectric constant at the water/surfactant interface increases as w_0 increases, reaching a plateau at $w_0 = 12$. They attribute this result to binding of water to the surfactant's polar headgroups. Correa et al.,[34] investigating the micropolarity of water in AOT reverse micelles, observed an increase in polarity with increasing water content up to $w_0 = 10$.

Several research groups have investigated the dynamical response of water in AOT reverse micellar systems. Zhang and Bright[24] investigated the reorganization of water in the interior of AOT reverse micelles on the nanosecond time scale using fluorescence spectroscopy of 1,8-anilino-8-naphthalenesulfonic acid (ANS). For $w_0 < 2.5$, they observed two relaxation processes with time constants of 0.5−1.7 and 3.5−11.8 ns that they attributed to "free" and "bound" water reorganization, respectively. For $w_0 > 2.5$, a single reorganization process with a time constant of 0.8−1.2 ns was reported. In general, they found that the observed rate constants decreased with increas-

* Corresponding author. E-mail: levinger@lamar.colostate.edu.

S1089-5647(97)03330-0 CCC: $15.00
Published on Web 03/20/1998

ing w_0. Cho et al.[35] have also probed the AOT interior using ~50 ps time-resolved fluorescence of ANS and suggest that the water molecules near the surfactant interface are icelike owing to the strong interactions with the polar-headgroup surface of high curvature and that the molecules appear bulklike ~6−18 Å from the interface. Sarkar et al.[36,37] performed time-resolved fluorescence measurements of a probe in micellar solutions and observed fluorescence decay with time constants ranging from 1.7 to 12 ns. They also attributed these dynamical changes to relaxation processes of water molecules in various environments of the water pool. Recently, Mittleman et al. have used ultrafast terahertz spectroscopy to probe the dielectric relaxation of water in Aerosol OT reverse micelles.[38] Both the time scale and amplitude of the relaxation were smaller than those of bulk water and were attributed to reduced long-range collective behavior resulting from the small water pool in the reverse micelles.

Of the many dynamical responses possible in the AOT reverse micelles, the response of intramicellar water should be the fastest. The dynamical characteristics of the AOT reverse micellar environment have been shown to include components on the picosecond and nanosecond time scales. However, the dynamics of polar solvent motion in bulk water[1] are considerably faster. Jimenez et al.[1] reported that 48% of the water solvent response occurs within 50 fs. The remaining solvation components are reported to have time constants of 126 and 880 fs. Because static characterization of AOT reverse micelles suggests the presence of bulk water, to compare motion in the reverse micelles directly with results in bulk water, it is imperative to know whether there are contributions to solvent motion in reverse micelles on similar ultrafast time scales.

The dynamical response of water inside reverse micelles can be investigated via polar solvation dynamics experiments. Polar solvation dynamics is the measure of the polar solvent response to an instantaneous change of the charge distribution in a probe molecule. Solvation dynamics of a wide variety of bulk liquids have been well studied both experimentally and theoretically.[39] These studies have revealed two different types of solvent motion: an ultrafast time scale component (<100 fs) attributed to an inertial solvent response, and a slower component (hundreds of femtoseconds to picoseconds) due to diffusive, solvent motion in response to the probe's new charge distribution. For bulk water, Jimenez et al.[1] have shown that the response, complete within 50 fs, is due to inertial solvent motion, while the two subpicosecond time constants are attributed to diffusive motion.

With the development of femtosecond lasers, even the ultrafast solvent motion can be experimentally observed using several different spectroscopic techniques.[40−46] Time-resolved fluorescence-upconversion spectroscopy utilizes the ultrashort pulses from these lasers.[40,41] This technique experimentally measures polar solvation dynamics by recording the changes in fluorescence, that is, the dynamic Stokes shift in fluorescence displayed by a fluorescent probe molecule over time.[40−42,47] Rigid probe molecules, such as coumarin dyes,[48,49] are used to ensure that the observed time-dependent fluorescence Stokes shift can be attributed to solvation without contributions from the probe's internal degrees of freedom. The collected data are analyzed by reconstructing the fluorescence spectrum over the time period of the dynamic Stokes shift. By use of the reconstructed time-resolved fluorescence spectra, the time-correlation function $C(t)$ can be calculated as

$$C(t) = \frac{\nu(t) - \nu(\infty)}{\nu(0) - \nu(\infty)} \tag{2}$$

where $\nu(t)$, $\nu(0)$, and $\nu(\infty)$ are identifiable features of a reconstructed spectrum (typically the peak) in wavenumbers at time t, instantaneously, and at equilibrium, respectively.[39,48,49]

In addition to measuring water motion in reverse micellar solutions via polar solvation dynamics experiments utilizing time-resolved fluorescence spectroscopy, molecular dynamics simulations suggest that this technique is sensitive to solvation dynamics at interfaces. Michael and Benjamin[50] have investigated the dynamics of solvents at a polar/nonpolar interface. They found that at a 50/50 water/octanol interface the solvent response occurs on a subpicosecond as well as picosecond time scale. In comparison, the relaxation rate observed one monolayer into the octanol layer, ~5 Å, is more than 2 orders of magnitude slower. These results suggest a probe molecule not only would be sensitive to solvation dynamics at interfaces but would also probe the nature of the interface.

Ultrafast solvation dynamics of water in the restrictive environment of the γ-cyclodextrin inclusion complex has been investigated by Vajda et al.[51] They observed the short-time components of the solvent motion typical of bulk water. These ultrafast solvent relaxation processes constituted approximately 90% of the total solvent response. The remaining solvation dynamics were observed to have time constants of 13, 109, 1200 ps. They attribute these slower solvent relaxation processes to motion of the entire complex rather than individual water motion.

Although work has begun to investigate water in restricted environments, namely, reverse micelles,[36,52] cyclodextrin/water complexes,[51] zeolites,[53] and sol−gel pores,[54,55] many questions are still left unanswered. For example, do solvation dynamics occur on an ultrashort time scale in any given restrictive environment? How does the restricted environment influence the water molecules and hence affect the solvation dynamics? In this paper, we present results from ultrafast solvation dynamics of water in AOT reverse micelles. We compare dynamics in reverse micelles of varying size, contrasting our results with bulk-water dynamics, predictions from static spectroscopy, and studies of water in other restricted environments.

Experimental Methods

Sample Preparation. Reverse microemulsions were prepared with isooctane (2,2,4-trimethylpentane, HPLC grade, Aldrich), Aerosol-OT (sodium bis(2-ethylhexyl)sulfosuccinate, Aldrich) and high-purity water (Milli-Q filtered, 18.2 MΩ/cm^2 resistivity). All were used without further purification. Electrospray mass spectrometry of the AOT revealed no contamination by other species. Karl−Fisher titration results showed that the AOT contained 0.617% water by weight or 0.15 water molecules per AOT molecule. The solutions for a given w_0 were prepared by weight with volume fractions of <0.25 to ensure that the micelles were monodisperse in solution.[56] The volume fraction of the sample is defined as

$$\phi = \frac{V_{H_2O} + n_{AOT}(v_{AOT} + n_{H_2O}v_{H_2O})}{V_{total}} \tag{3}$$

where V_{H_2O} is the volume of water, n_{AOT} is the number of moles of AOT, v_{AOT} is the volume of one AOT molecule (0.39 dm^3/mole),[57] n_{H_2O} is the number of water molecules per AOT molecule, v_{H_2O} is the volume of one H_2O molecule, and V_{total} is

the total volume of the solution. The diameters of the prepared reverse micelles were measured using a Coulter N4Plus commercial PCS spectrometer as described previously[58] and correspond well with literature values.[56,59−61] Bulk water samples at pH 9 were prepared with NaOH (reagent grade, Fisher). Solutions of 1 M Na^+ at pH 9 were prepared with Na_2SO_4 (reagent grade, Fisher).

The anionic laser dye coumarin 343 (C343) was purchased from Exciton and used without further purification. This dye is soluble in water and highly insoluble in hydrocarbons; absorption spectra of C343 in isooctane show no dye present. Via a spectrophotometric titration, we have measured the pK_a to be ∼4.5. C343 was added in excess to the prepared samples. The samples were periodically shaken manually and sonicated for 1−5 min over a 24−48 h period and then filtered to remove any excess dye. Via ground-state absorption spectra collected with a Cary 2400 UV/vis/IR spectrophotometer, we estimate that the concentration of dye is at most one C343 molecule per 50 micelles. This ensures that the measured spectroscopy and dynamics arise from individual C343 molecules rather than from molecular aggregates. Fluorescence-emission spectra were collected with a home-built fluorometer.[62] Fluorescence lifetimes were determined by time-correlation single-photon-counting (TCSPC) measurements using a home-built instrument with excitation pulses centered at 315 nm and with an instrument response function of 90 ps (fwhm).[63]

Fluorescence-Upconversion Spectroscopy. The femtosecond fluorescence-upconversion spectrometer used to collect time-resolved fluorescence signals is similar to the apparatus designed by Fleming and co-workers.[64] The excitation source is a mode-locked Ti:sapphire laser (NJA-3, Clark) pumped by all lines of an Ar^+ laser (Innova 310, Coherent) at 6.5 W. The Ti:sapphire laser produces output pulses with 80 fs duration (fwhm assuming $sech^2$ pulse shape) at a 100 MHz repetition rate and with energies of 5−6 nJ/pulse. The spectrum of the pulses was centered at 800 nm. Divergence of the output is corrected using a 1.5 m focal length lens (fused silica) and a telescope consisting of a 15 cm negative lens and a 20 cm positive lens (both AR-coated). The resulting collimated beam has a diameter of 2−5 mm. The collimated beam is then frequency-doubled in a 1 mm barium borate crystal (BBO, type I, INRAD). The frequency-doubled pulses are separated from the fundamental using a dielectric beam splitter (CVI). These pulses are sent through an optical delay line equipped with a motorized delay stage (Parker-Daedl delay stage, American Precision step motor), passed through a $\lambda/2$ plate (400 nm center wavelength, Meadowlark Optics), and focused by a 10 cm lens into a 1 mm quartz flowing sample cell. A small cone of the forward fluorescence is collected and focused with an ellipsoidal rhodium reflector (Melles Griot) into a nonlinear crystal (BBO, type I, 0.5 mm thick, Casix). The fluorescence is upconverted with the residual fundamental pulses that have been passed through a $\lambda/2$ plate (780 nm center wavelength, Meadowlark Optics) and focused onto the BBO upconversion crystal with a 10 cm lens. All solvation dynamics measurements were made with parallel polarization of the excitation beam with respect to the gate beam. The upconverted light was collimated by a 10 cm lens (2 in. diameter, fused silica), isolated from the gate and fundamental beams using an iris, and dispersed by a Brewster prism (fused silica, CVI). The upconverted beam is then focused with a 12.8 cm lens (fused silica) through a UV-transmitting filter (340 nm, Opto-Sigma) into a 0.33 m single monochromator (HR320, ISA) equipped with a 2400 grooves/mm grating blazed at 400 nm. The bandwidth of the fluorescence detected at a single wavelength was on the order of 8 nm. The overall instrument response as determined from the cross correlation of the excitation and gate pulses in the BBO crystal is 175−185 fs (fwhm, assuming a Gaussian line shape). The upconverted photons are detected using a photomultiplier tube (PMT, R4220, Hamamatsu) in a cooled housing (TE177RF, Products for Research). The signal is then amplified using two video amplifiers (CLC100, Comlinear Corporation) in series and digitized by a two-channel photon counter (SR400, Stanford Research Systems). A personal computer using LabVIEW (National Instruments) routines collects the photon counter signals as a function of optical delay between the excitation and gate pulses. Fluorescence-upconversion measurements were obtained by counting for 1 s at each delay. Each transient is the average of 4−8 scans.

For all fluorescence-upconversion measurements, samples (∼200 mL volumes) were circulated through the cell using a low-flow cavity-style pumphead equipped with an electric motor (Micropump). Samples typically had an absorbance of 0.12−0.8 at 400 nm, as measured in a 1 mm quartz cell, and exhibited no degradation over the course of the experiment.

Data Analysis. The spectral reconstruction method was employed to determine the time-correlation functions $C(t)$ for water in the various micellar environments.[48,49] Briefly, the time-resolved fluorescence-upconversion decays were fit to multiexponential functions using an iterative reconvolution analysis program. A Gaussian function fit to the cross-correlation signal of the pump and gate pulses was used as the instrument response function. The resulting deconvolved functions for given fluorescence wavelengths were normalized at long time delay (typically greater than 10 ps) to the corresponding steady-state fluorescence-emission spectrum. This time delay was found to be adequate to ensure the correct spectral shape of the spectra at short time delays.

We then constructed the time-resolved fluorescence spectra from the normalized fits of the fluorescence-upconversion signals. The resulting spectra were parametrized in terms of the peak maximum ($\nu(t)$), spectral width ($\Delta\nu(t)$), and a factor to account for the asymmetry of the line shape (ρ) by fitting the spectra to log−normal line shapes.[65] The time-correlation function, tcf (see eq 2), was calculated with the peak maximum at various gate delays $\nu(t)$; $\nu(0)$ is the peak of the reconstructed fluorescence-emission spectrum at 0 fs delay and $\nu(\infty)$ is the peak of the steady-state fluorescence-emission spectrum. We would have liked to estimate $\nu(0)$ as previously discussed by Fee and Maroncelli;[66] however, the unique environment of the reverse micelles precludes this type of estimation.

Results and Discussion

We have investigated the polar solvent response of water in AOT reverse micelles using C343 as the molecular probe. Figure 1 shows the absorption spectra of C343 in these differently sized micelles as well as in bulk water. Upon solubilization of C343 in the reverse micelles, the spectrum shifts to shorter wavelength with respect to the spectrum of C343 in bulk water. This indicates that the environment sampled by the dye within the micelles differs from that of bulk water. The absorption spectrum of C343 in the smallest micelles, $w_0 = 1.1$, peaks at ∼20 nm to the blue of the dye peak in bulk water. As the micellar size increases, the spectrum shifts smoothly to longer wavelength. The static fluorescence-emission spectrum exhibits a similar shift. An isosbestic point is not observed in either the absorption or the fluorescence-emission spectra, suggesting that the observed shifts do not arise from two

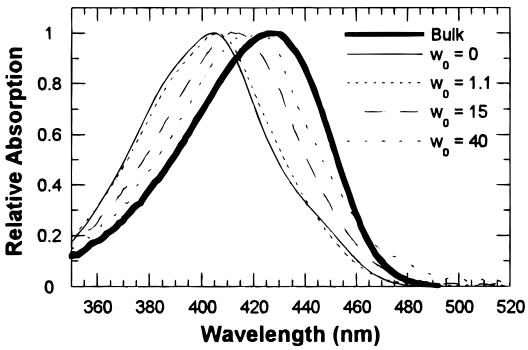

Figure 1. Ground-state absorption spectra of C343 in bulk water and various AOT reverse micellar environments at ambient temperature (22 °C).

different forms of the dye, such as protonated and deprotonated, either in the ground or in the excited state. The spectral shift observed with increasing w_0 indicates that the dye is sensitive to the micelle water loading. However, even for the largest micelles probed, $w_0 = 40$, the C343 absorption spectrum has not achieved the red shift associated with the spectrum in bulk water. Here, we estimate ≥10 000 water molecules are solubilized inside the micelle, sufficient to present a bulklike environment. This suggests that the probe molecule resides in an environment different from that of bulk water.

Because C343 is so insoluble in the alkane phase owing to the carboxylic acid group, we are confident that the dye does not reside outside the micelles or even amidst the alkyl tails of the surfactant. However, the probe may reside intercalated between surfactant headgroups rather than completely in the aqueous phase.

To investigate the location of the probe molecule in the micellar interior, we have used time-resolved fluorescence depolarization of C343 in 1 M Na^+ solution and various micellar environments. Time-resolved fluorescence anisotropies, $r(t)$, were calculated using eq 4:

$$r(t) = \frac{I_{||}(t) - I_{\perp}(t)}{I_{||}(t) + 2I_{\perp}(t)} \tag{4}$$

where $I_{||}(t)$ and $I_{\perp}(t)$ are the time-resolved fluorescence-upconversion signals obtained using excitation and gate pulses with parallel and perpendicular polarization, respectively. These fluorescence-upconversion signals were used without deconvolution, since the rotational motion of C343 in the various environments occurs on a time scale much longer than the instrument response function. Additionally, since the depolarization time scales for C343 in the various environments are significantly longer than the time scales measured for the solvation dynamics in the reverse micelles, the fluorescence-upconversion data obtained using parallel polarization conditions do not bias the solvation dynamics results.

Figure 2 shows the resulting anisotropy data, which fit well to biexponential decay functions as reported in Table 1. For C343 in 1 M Na^+ solution, >90% of the fluorescence depolarization occurs within 200 ps. This time scale is comparable to rotational motion of coumarin 153 in various polar solvents.[67] The rotational motion of C343 inside the micelles occurs at much slower rates. For $w_0 = 1.7$, fluorescence depolarization is measured to have a time constant of 1.3 ns, the same time scale as micellar rotation measured via ESR.[68] As w_0 increases, a small depolarization component is observed on the time scale of C343 in bulk electrolyte, the remainder occurring on the same time scale as observed for micellar rotation. These results show

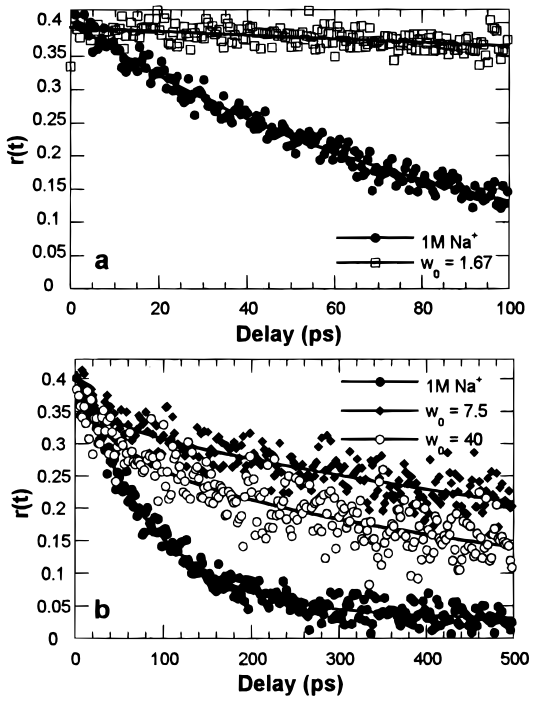

Figure 2. Time-resolved fluorescence anisotropy: (a) water/AOT/isooctane reverse micelles, $w_0 = 1.1$ (□), and 1 M aqueous Na^+ (●) (b) water/AOT/isooctane reverse micelles, $w_0 = 7.5$ (◆) and 40 (○), and 1 M aqueous Na^+ (●). Values for the fits are given in Table 1.

TABLE 1: Fit Parameters of the Time-Resolved Anisotropy Measurements

sample	w_0	c_1	τ_1 (ps)	c_2	τ_2 (ns)
1 M Na^+ solution		0.37 ± 0.01	83 ± 4	0.03 ± 0.10	1.2 ± 1.1
reverse micelles	1.7			0.4 ± 0.01	1.3 ± 0.1
	7.5	0.04 ± 0.01	75 ± 36	0.34 ± 0.01	1.2 ± 0.1
	40	0.10 ± 0.02	66 ± 27	0.27 ± 0.02	0.8 ± 0.1

that the probe molecule is intimately associated with the micelles and resides at the micellar interface near the AOT headgroups. Additionally, the magnitude of the picosecond component increases and the slower component time constant decreases as w_0 increases. This indicates that the rotational motion of C343 in the largest reverse micelles, $w_0 = 40$, is faster than in the smaller micelles and the probe molecule experiences a decreasingly restrictive environment with increasing micelle size. However, it is still clear that, even in the largest micelles probed, the dye molecules do not sample a bulklike environment.

Bulk Solvation Dynamics. As a baseline for our solvation dynamics measurements, we have repeated fluorescence-upconversion measurements of C343 in bulk water as reported by Jimenez et al.[1] Figure 3 shows the reconstructed time-resolved fluorescence-emission spectra we have obtained for C343 in water at pH 9. We performed these experiments at pH 9 to ensure that the dye was in the anionic form. Figure 3 also shows the experimentally determined tcf for bulk water generated from the reconstructed spectra. The instrument response of our fluorescence-upconversion apparatus, 175 fs, precluded us from observing the ultrafast inertial component of the solvent response. However, we do observe subpicosecond diffusive components. The time constants of these components were found to be 0.22 ps (29%) and 0.59 ps (71%) as shown in Table 2. These time constants are on the same time scales as reported by Jimenez et al.,[1] where the relative diffusive components are 126 fs (36%) and 880 fs (63%).[91] Vajda et

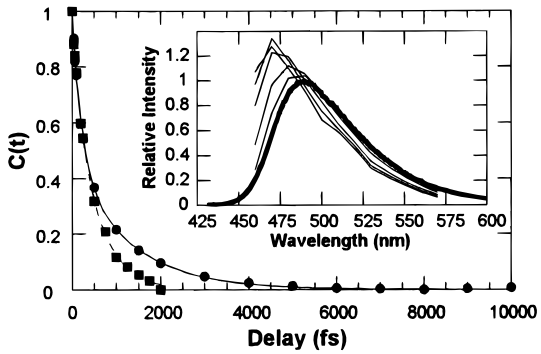

Figure 3. Time-correlation functions, $C(t)$, for bulk water (■) and 1 M Na^+ solution (●) at ambient temperature (22 °C) and pH 9. The tcf's were fit to $C(t) = \sum_i [a_i \exp(-t/\tau_i)]$. Values for the fits are given in Table 2. Inset: Reconstructed time-resolved fluorescence-emission spectra for bulk water at time delays of 50, 100, 200, 500, 1000, and 2000 fs (peak moving left to right, respectively) and steady-state fluorescence-emission spectrum (thick curve) of C343 in bulk water at ambient temperature (22 °C) and pH 9.

al.[51] and Jarzeba et al.[69] have also reported similar solvation dynamics for bulk water using different coumarin probe molecules.

Recently, Zolotov et al.[70] have also investigated the solvation dynamics of bulk water using heterodyne optical Kerr spectroscopy in resonance with two probe molecules, rhodamine 800 and 3,3′-(diethylthia)tricarbocyanine bromide. They observed a bimodal solvent response with a sub-100 fs inertial component and a picosecond, diffusive component. However, the time constants for both components are slower than previously reported.[1,51,69] In particular, the picosecond component, with a 6.8 ps time constant, is significantly slower than the time constants we measured and those reported by Jimenez et al.[1] Zolotov et al.[70] attributed the slower dynamics to the dipolar nature of the probe molecules. They base this result on recent computer simulations performed by Nandi et al.[71] who showed that solvation of a dipolar molecule occurs at a slower rate than solvation of a similar-sized ionic probe. However, Nandi et al.[71] calculated a tcf for bulk water that agrees well with that reported by Jimenez et al.[1] Furthermore, experimental results reported by Vajda et al.[46] for coumarin 480, a dipolar probe, agree with our results and the results of Jimenez et al.[1] even though the C343 probe molecule is ionic. Consequently, the long time scale diffusive component measured by Zolotov et al.[70] may be due to other factors and are not directly comparable to this work.

Comparison of water dynamics in bulk and in reverse micelles, however, may not be warranted, since the micellar interior is strongly electrolytic. Therefore, we have also investigated the effects of an electrolyte on water dynamics. Figure 3 contrasts the tcf for 1 M Na^+ (Na_2SO_4) aqueous solution at pH 9 with the bulk-water dynamics. The tcf fits well to a biexponential decay with time constants of 0.21 ps (54%) and 1.3 ps (46%) (see Table 2). The faster of the two components is on the time scale of the initial diffusive component measured for bulk water, while the second component is significantly longer.

Solvation dynamics in nonaqueous ionic solutions with a range of ion concentrations have been previously reported.[72−75] These studies employed TCSPC, hence the time resolution limited the response to >50 ps features. The dynamics measured for these solutions contained additional slow components compared to the dynamics in pure solvents. Both analytical theoretical studies and computer simulations have been used in order to examine the effects of ions on the dynamics of the solvent. Chandra and Patey[76] developed a microscopic theory of ion solvation in electrolyte solutions. They showed that the short time dynamics are governed by an inertial response very similar to that observed in pure solvents. At long times, there is an additional feature not present in pure solvents postulated to arise from ion−ion relaxation. Chandra[77] has also made a detailed study of the solvation dynamics dependence on salt concentration. This work showed that the inertial component of the dynamics depends only weakly on the salt concentration, indicating that it arises from the solvent motion, while the long-time delay depends strongly on the amount of salt in solution. This long-time component also showed a dependence on the organization of the ion atmosphere. Neria and Nitzan,[78,79] employing molecular dynamics simulations, have also modeled solvation dynamics in electrolytic solutions. Their simulations confirmed that the slow dynamical component observed in experiments arises from ion-exchange interactions between the first solvation shell and the solute. The simulations also revealed a high degree of correlation between the motion of the ions and the solvent molecules. Molecular dynamics calculations have also shown that the presence of sodium ions in water decreases the water mobility.[80,81]

To investigate the slower solvation dynamics in aqueous solutions, we have measured time-resolved fluorescence-upconversion signals over a 500 ps time scale and TCSPC signals over a 8 ns time scale for C343 in the various solvent environments. The 500 ps fluorescence measurements for C343 in bulk water fitted to multiexponential decay functions reveal a fluorescence decay component with a time constant of 72−77 ps in addition to the subpicosecond components. We attribute this component to a slow solvent reorganization process. A similar spectral change is observed in the fluorescence of C343 in the 1 M Na^+ solution but on a longer time scale with a time constant of 103−128 ps. This suggests that water dynamics are slowed in salt solutions because of the interaction of water molecules with the ions as discussed above. The slower component observed for bulk water may also be attributed to the interaction of water with Na^+ as the bulk water was adjusted to pH 9 using sodium hydroxide. The TCSPC data were also fit to a multiexponential decay function that shows the lifetime of the excited state S_1 of C343 in these solvent environments is 4.5 ns.

Solvation Dynamics in H_2O/AOT/Isooctane Reverse Micelles. In comparison with the bulk-water dynamics, time-resolved fluorescence measurements of C343 in the AOT reverse micelles reveal significant differences. Perhaps the most striking difference is the dynamics measured for the smallest micelles, $w_0 = 1.1$. Figure 4a displays the time-resolved fluorescence-upconversion data for C343 in these micelles detected at various wavelengths. On the 2 ps time scale the fluorescence transients at the different wavelengths look identical; essentially no change in the fluorescence is observed. Figure 4b shows the reconstructed time-resolved fluorescence-emission spectra. These spectra were normalized with respect to the steady-state fluorescence-emission spectrum at a time delay of 2 ps. Within 500 fs, the reconstructed time-resolved spectra show a Stokes shift of only 40 cm^{-1} with the remaining approximately 60 cm^{-1} Stokes shift occurring on >100 ps and longer time scale. The total dynamic Stokes shift observed for C343 in this sample is 100 cm^{-1}, in contrast to bulk solvent where we observe a Stokes shift of ∼1000 cm^{-1}.

The main spectral change observed in the reconstructed time-resolved spectra shown in Figure 4b is an increase in area of

TABLE 2: Fit Parameters of the Ultrafast Components of the Solvent-Correlation Functions for Water in Various Reverse Micellar Environments

sample	w_0	ϕ	micellar diameter[a] (Å)	no. H_2O in pool	Stokes shift[b] (cm^{-1})	$C(t)$ c_1	τ_1 (ps)	c_2	τ_2 (ps)
bulk water					965	0.29	0.22	0.71	0.59
1 M Na^+ soln					823	0.54	0.21	0.46	1.3
reverse micelles	1.1[c]	0.17	32 ± 4	~25	50				
	5[d]	0.10	~90		220	0.43	0.25	0.57	3.3
	7.5[e]	0.15	90−100		390	0.69	0.11	0.31	3.0
	15[e]	0.20	101 ± 1		425	0.68	0.24	0.34	2.9
	40[e]	0.21	205 ± 3	~10^5	485	0.57	0.16	0.43	2.2

[a] Diameter of micelles measured using dynamic light scattering as previously reported.[50] [b] Observed Stokes shift over the first 10 ps. [c] Reconstructed time-resolved fluorecence emission spectra normalized at a time delay of 2 ps with respect to the steady-state spectrum. [d] Reconstructed spectra normalized at a time delay of 20 ps with respect to the steady-state spectrum. [e] Reconstructed spectra normalized at a time delay of 10 ps with respect to the steady-state spectrum.

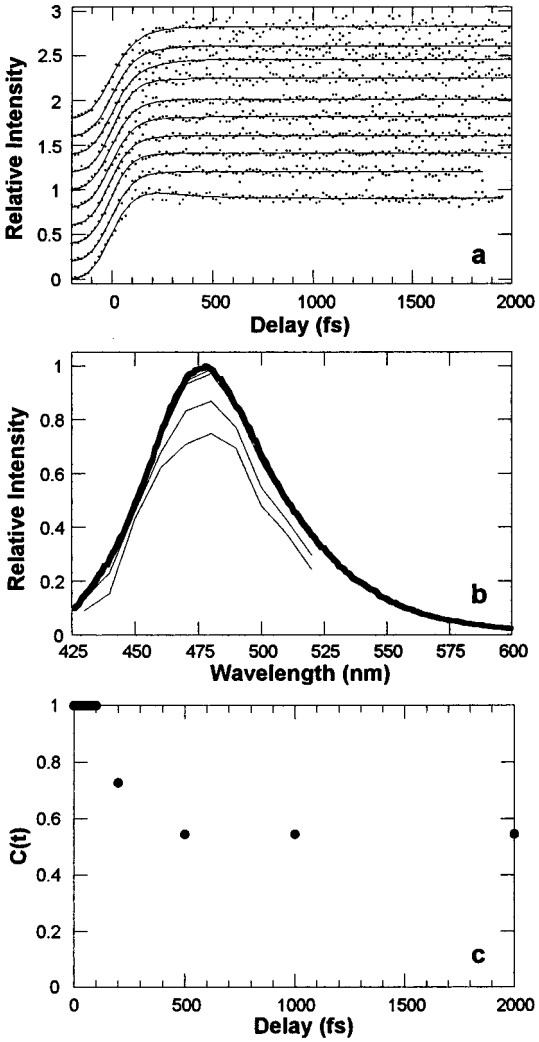

Figure 4. (a) Femtosecond fluorescence-upconversion data for C343 in AOT reverse micelles with $w_0 = 1.1$ at ambient temperature (22 °C) detected from 430 nm (bottom trace) to 520 nm (top trace) in 10 nm steps. Each transient is normalized to 1 and shown offset for clarity. (b) Reconstructed time-resolved fluorescence-emission spectra at time delays of 50 fs (bottom spectrum) to 2 ps (top spectrum) and steady-state fluorescence-emission spectrum (thick curve) of C343 in AOT reverse micelles, $w_0 = 1.1$. (c) Solvation dynamics time-correlation function, $C(t)$, for water in AOT reverse micelles, $w_0 = 1.1$.

the spectrum as a function of time rather than a spectral shift. The origin of this spectral change is unclear. It may be due to vibrational relaxation processes, including intramolecular vibrational redistribution (IVR), of the excited C343. For bulk solvation dynamics experiments using rigid coumarin dyes, IVR relaxation processes have not been observed in the time-resolved fluorescence Stokes shift because the resulting spectral changes are minuscule compared with the spectral changes associated with the solvation dynamics.[42] Another possible explanation for the observed spectral changes may be that the dye is excited to a higher-energy excitation state that does not display prompt fluorescence.[82] However, there is no evidence that this is the case for coumarin dyes in bulk polar solvents,[42] and the static spectra of C343 do not indicate significantly different electronic structures present within the micelles.

Figure 4c shows the tcf for water in AOT reverse micelles, $w_0 = 1.1$. The tcf is essentially invariant for the first 200 fs and then takes a modest step down, after which the majority of the decay measured occurs on the time scale of the fluorescence lifetime, 4.5 ns. We cannot fit the tcf to any reasonable function. We interpret these results, that is, the minuscule Stokes shift and $C(t)$ function that does not follow a functional form, to indicate that the water molecules are effectively immobilized in these micelles.

In contrast to the small-size AOT reverse micelles, water in larger AOT reverse micelles is not completely immobilized. Parts a and b of Figure 5 show the reconstructed fluorescence-emission spectra of C343 in AOT reverse micelles with $w_0 = 5$ and time delays ranging from 0 fs to 20 ps (Figure 5a) and from 20 to 400 ps (Figure 5b). These data were obtained using the sodium salt of C343.[83] The reconstructed spectra were normalized to the steady-state fluorescence-emission spectrum at time delay of 400 ps. Within the first 20 ps, Figure 5a, we observe a fast spectral shift to the red and an increase in the relative intensity of the fluorescence-emission spectra. On a much longer time scale, shown in Figure 5b, we observe a continuing shift of the spectra to the red and a decrease in the relative fluorescence-emission intensity on the time scale of the lifetime of the dye. Figure 6a shows the tcf determined from these reconstructed spectra. For all the micelles measured, we observe no inertial solvent motion due to the time-resolution of our experiments. The tcf fits well to a multiexponential decay function with time constants of 0.33 ps (19%), 6.5 ps (19%), and 129 ps (62%). Hence, for a fairly small increase in the amount of water in AOT reverse micelles, not only is the solvation dynamics faster than that observed for the reverse micelles with $w_0 = 1.1$, but also we observe a subpicosecond component on a time scale similar to diffusive water motion in bulk solvent.

Because the identifiable water motion occurs on a time scale of less than 20 ps, we have also determined the tcf for the AOT reverse micelles with $w_0 = 5$ using reconstructed time-resolved fluorescence-emission spectra normalized at a time delay of 20 ps with respect to the steady-state fluorescence-emission

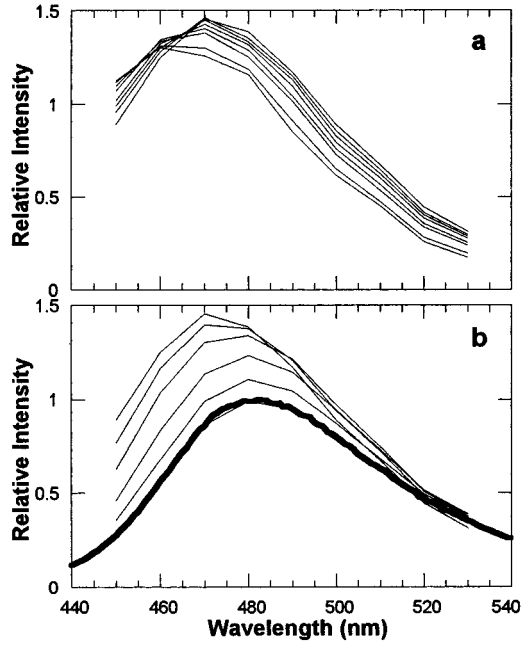

Figure 5. Reconstructed fluorescence-emission spectra of C343 in AOT reverse micelles, $w_0 = 5$, at ambient temperature (22 °C) at time delays of (a) 0, 0.1, 0.5, 1, 3, 6, 10, and 20 ps (peak moving left to right, respectively) and (b) 20, 50, 100, 200, 300, and 400 ps (peak moving left to right, respectively) and the steady-state fluorescence-emission spectrum (thick curve).

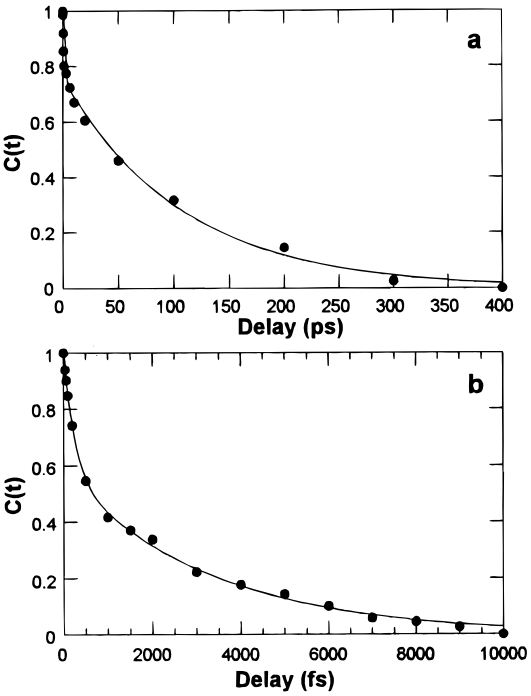

Figure 6. Time-correlation functions, $C(t)$, for water in AOT reverse micelles, $w_0 = 5$, generated from the data in Figure 4 showing the effect of normalizing at different time delays. Reconstructed spectra normalized at (a) 400 ps and (b) 10 ps.

spectrum. These spectra exhibited spectral changes similar to those observed in Figure 5a. Figure 6b shows the tcf determined from the reconstructed spectra normalized at 20 ps and fit to log−normal line shapes. The resulting tcf fits well to a biexponential decay function with time constants of 0.22 fs (43%) and 3.3 ps (57%) (see Table 2). These time constants and relative magnitudes with respect to each other are quite similar and directly comparable to the time constants observed

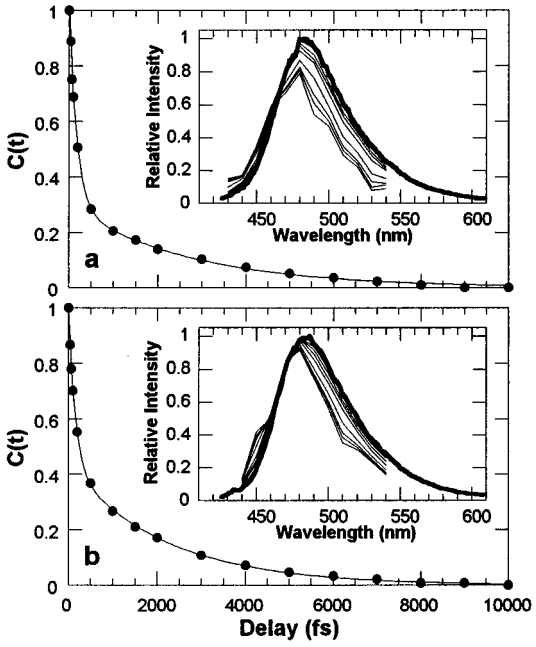

Figure 7. Time-correlation functions, $C(t)$, and multiexponential fits for water in AOT reverse micelles with (a) $w_0 = 15$ and (b) $w_0 = 40$. Values for the fits are given in Table 2. Inset: Reconstructed time-resolved fluorescence-emission spectra for bulk water at time delays of 33, 67, 100, 200, 500, 1000, 2000, 5000, and 10 000 fs (peak moving left to right, respectively) and steady-state fluorescence-emission spectrum (thick curve) of C343 in the respective reverse micelles.

for the tcf shown in Figure 6a without the longer time constant component. Hence, we conclude that the time-resolved reconstructed spectra normalized on a tens of picosecond time delay can be used to determine the tcf over the time scale to which the spectra were normalized. Additionally, the long-time component of the solvation dynamics can be estimated by the fluorescence decay at the peak of the equilibrium fluorescence.[84,85]

We have also investigated the solvation dynamics in larger AOT reverse micelles, $w_0 = 7.5$, 15, and 40. The reconstructed time-resolved spectra for these samples were normalized at a time delay of 10 ps with respect to the steady-state fluorescence-emission spectra because the solvent relaxation was essentially complete. Parts a and b of Figure 7 show the plots of the tcf for micelles with $w_0 = 15$ and 40, respectively. As shown in Table 2, the tcf for these samples decays with two characteristic lifetimes. Like the AOT reverse micelles with $w_0 = 5$, the fastest time constant of the fitted tcf for micelles with $w_0 = 7.5$, 15, and 40 is on a time scale similar to the faster diffusive water motion in bulk solvent, 110−240 fs. The slower time constant for these micelles is on a time scale significantly longer than observed in bulk water or 1 M Na^+ solution. Additionally, this time constant decreases as w_0 increases.

To compare the relative water mobility in the various micellar environments, we have calculated the unnormalized solvation function $S(t)$,

$$S(t) = \nu(t) - \nu(0) \tag{5}$$

where $\nu(t)$ and $\nu(0)$ are the peak of the reconstructed spectrum in wavenumbers at time t and instantaneously. $S(t)$, shown as a function of time in Figure 8, contrasts the relative magnitudes of the Stokes shifts of C343 in the various environments as well as the relative relaxation rates. For $w_0 = 1.1$, the minuscule Stokes shift shows that there is essentially no solvent motion within 10 ps. As w_0 increases, both the magnitude of the Stokes

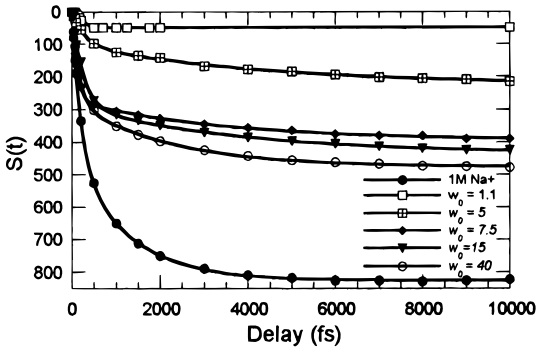

Figure 8. Unnormalized time-correlation functions, $S(t)$, showing the magnitude of the overall Stokes shift in addition to the dynamic response for water in AOT reverse micelles, with $w_0 = 1.1$ (□), 5 (crossed squares), 7.5 (◆), 15 (▼), and 40 (○), and for bulk water (●).

shift and the relaxation rate increase. However, even for the largest micelles, $w_0 = 40$, neither the overall Stokes shift nor the relaxation rates have reached the magnitude observed in the bulk salt solution.

We attribute the solvation dynamics we observe in the AOT reverse micelles larger than $w_0 = 1.1$ to increased solvent mobility as the micellar interior expands. As w_0 increases, the core water pool grows, leaving proportionately less water bound to the micellar interface. Hence, the observed dynamics are faster, although translational motion of the water is still restricted by the size of the micelle. The two decay components of the tcf may be attributed to two different water environments. We attribute the faster component to solvation dynamics of the inner "bulk" pool water molecules. This component decays on the same time scale as that of the faster diffusive component of bulk water.[1] The slower component observed in these reverse micelles is attributed to the water molecules that interact with the micellar interface. The time scale of the slower component decreases as w_0, or the water pool size, increases, suggesting that the number of water molecules bound to the interface decreases. However, it is also possible that a part of the observed decrease may be due to the average location of the probe molecule moving away from the micellar interface as indicated by our anisotropy measurements.

For all reverse micelles investigated, we observe a subnanosecond decay component in addition to the subpicosecond and picosecond components. This decay component ranges from 200 to 400 ps in the time-resolved fluorescence-upconversion signals, similar to decays for C343 in bulk water and 1 M Na^+ solution. This subnanosecond time constant is observed to decrease as w_0 increases. Interestingly, even for $w_0 = 40$, this component is not as fast as observed in bulk water or 1 M Na^+, which suggests that it reflects collective motion of the surfactant and water at the micellar interface.

Solvation dynamics observed for water inside a γ-cyclodextrin cavity[51] reveal results that are similar to the results for AOT reverse micelles reported here. The γ-cyclodextrin cavity probed has an inner diameter of 8.3 Å and is hydrophobic owing to hydroxide side chains. This cavity is the same size as the AOT reverse micelles with $w_0 \approx 1$.[56] Cyclodextrins are known to complex with small molecules. Vajda et al.[51] reported solvent relaxation processes observed for a coumarin dye in a γ-cyclodextrin cavity. The measured dynamics include an inertial response with a $<$50 fs time constant and processes with 310 fs, 13, 109, and 1200 ps time constants. They attribute the subpicosecond relaxation process to diffusive water motion similar to that observed in bulk water. The dynamics associated with the longer time constants accounted for approximately 10% of the tcf and were attributed to reorientation of highly constrained water molecules, to motion of the inclusion complex due to the flexibility of the γ-cyclodextrin ring, and to possible motion of the probe molecule in to and out of the cyclodextrin. The water response in the γ-cyclodextrin/water complex has been modeled by Nandi and Bagchi[86] using continuum theory based on a multishell model and molecular hydrodynamics theory. In agreement with Vajda et al., they conclude that the short time dynamics are due to bulk-water motion and only the long time dynamics are affected by the restricted environment. However, they attribute the long-time components of the solvent response to a collective motion of the solvent involving hindered translational motion of water inside the cyclodextrin cavity. This work suggests that the slower relaxation components we observe in the tcf for the AOT micelles may arise from hindered water motion in the restricted micellar environment. However, it is likely that the motion we observe on the 129 ps time scale reflects collective water and micellar interfacial motion rather than exclusively water motion.

Sarkar et al. have recently used TCSPC to measure the solvation dynamics in water/AOT/heptane reverse micellar solutions via the time-resolved Stokes shift of coumarin 480 in solution.[36] Their experimental results differ from our work in several ways. In particular, because their probe is soluble in the nonpolar phase and insoluble in water, it is unlikely that observed changes in the fluorescence of the dye can be attributed solely to water motion. They report solvent motion occurring on the nanosecond time scale and that the time scale for this motion decreases as w_0 increases. Additionally, the time resolution for their apparatus is $>$50 ps. This precluded them from measuring any ultrafast motion, especially that of bulk water. Recently, Das et al.[52] investigated the deuterium isotope effect on proton transfer in AOT reverse micelles in heptane by measuring the time-resolved fluorescence emission of 4-aminophthalimide inside these micelles with $>$50 ps time resolution. They reported that solvation dynamics occurs on a time scale faster than could be observed with their instrumentation. However, for $w_0 = 12$, they observe a 500 ps solvation component that is on the same time scale as we observe for the slowest dynamics in our measurements.

Immobilization of solvents in restricted environments, such as sol−gel glasses, has been previously reported. Awschalom and Warnock[54] investigated the subpicosecond dynamics of nitrobenzene and carbon disulfide in 4.4 nm diameter pores by measuring the time-resolved birefringence signal of the solvents on a subpicosecond time scale. They found that the dynamics of solvent in the pores was directly related to the interaction of the solvent with the sol−gel surfaces; the polar solvent in contact with pore surfaces having −OH groups showed significantly slower dynamics than the solvent in pores with less polar group surfaces and nonpolar solvents in similar sol−gel glass pores. Streck et al.[55] used quinoxaline to measure the solvation dynamics of 2-methyltetrahydrofuran (MTHF) inside sol−gel glasses with 2.5, 5.0, and 7.5 nm pore diameters. The samples were cooled to 70−85 K, which is below the glass transition for MTHF. They observed that the solvent dynamics appeared to be separated into a very slow component associated with a surface layer of solvent molecules and a faster component attributed to an inner solvent pool. For the smallest-diameter pores, they observed only a very slow process similar to what we observe in the smallest AOT reverse micelles. The solvation dynamics study in sol−gel glasses with increasing pore size show trends similar to the trend we observe for micelles with increasing w_0.[55]

Comparison of these studies on the dynamics of solvents in sol−gel glasses with our micelle results strongly suggests that the immobilization of water in the small micelles, $w_0 = 1.1$, is due to a strong interaction of the water molecules with the surfactant interface. These interactions are most likely due to ion−dipole interactions of individual water molecules with the surfactant headgroup, a sulfonate group, or the surfactant's counterion, Na^+. Although other interactions such as dipole−dipole interactions with the succinate group and dispersive forces with the hydrocarbon tails could influence the dynamics, they should play only a minor role in freezing out the water motion.

Previous characterizations of the water pool in the reverse micelles using IR and NMR spectroscopy corroborate this interpretation and our results. IR spectroscopic studies show that water in AOT reverse micelles exists essentially in two forms: bound water due to molecules interacting strongly with the surfactant polar headgroups, and free water involved in a hydrogen-bonding network like that found in bulk.[25−33] The relative contributions from these two water types depend on the amount of water solubilized within the micelles. The exact amount of bound and free water differs in different studies. On the basis of spectral shifting of the sulfonate moiety, Christopher et al.[32] and Moran et al.[33] report that three to four water molecules bridge between the Na^+ and $-SO_3^-$ in AOT reverse micelles. This result is consistent with our dynamics measurements showing that the water in micelles with $w_0 = 1.1$ is completely bound, but by $w_0 = 5$ there already appears an ultrafast bulklike relaxation component. IR studies focusing on the nature of intramicellar water also show that as the water content inside the micelles increases, more and more hydrogen-bonding characteristics are observed in the spectra of the intramicellar water.[26−29] Again, this is consistent with our dynamics results showing a relaxation component due to bulklike water that increases with increasing micelle water loading. Finally, NMR studies reported by Maitra[19] suggest that the thickness of the bound layer decreases slightly as w_0 increases. This provides another explanation for our observation that the time scale for relaxation decreases as w_0 increases.

These conclusions are also supported by molecular dynamics simulations. Two different groups have performed simulations to investigate the molecular structure of the aqueous core in reverse ionic micelles. Brown and Clarke[87] modeled an aqueous reverse micelle in a nonpolar solvent using a cationic surfactant. They reported that the anions associated with the surfactant are tightly bound to the cation headgroup surface, although water molecules can significantly penetrate into the hydrophobic region. Additionally, water molecules at the interface interact strongly with the anions and therefore do not have bulklike characteristics. Linse[88] investigated the structure and dynamics of water in reverse micelles formed with an anionic surfactant similar to AOT. He reported that interactions of water molecules with the ionic headgroups of the surfactant interface essentially break the hydrogen-bonding network of the water and that although the hydrophobic portion of the interface plays a role in breaking this network, it is only a minor one. He also attributes the interaction of the water with sodium ions and anionic headgroup to reduced translational and rotational motion of water in the micellar environment.

The subnanosecond decay components observed in the fluorescence-upconversion signals could be attributed to the Na^+ ions present in the micellar environment. Ionic solvation dynamics have recently been studied using zeolites. Das et al.[53] investigated the solvation dynamics of ions in faujasite zeolite 13X, an aluminosilicate with a spherical supercage structure containing 8 Å diameter pores. They measured the changes in fluorescence with ~70 ps time resolution of a coumarin dye in this zeolite. They found that the time constants of the tcf were significantly slower than the time constants observed for the tcf of bulk liquids but similar to those in ionic solutions. They attribute these results to solvation by Na^+ ions present in the zeolite as well as motion of the probe within the zeolite pores. This result supports our conclusions that slow dynamical processes in the AOT reverse micelles as well as in the Na^+ solution are due to the interaction of water with Na^+ ions.

To probe the role of the counterions in immobilizing water inside AOT reverse micelles, we have recently exchanged the sodium cation normally complexed to the AOT for an ammonium cation.[89] In this study, we probed the solvation dynamics in reverse micelles of the same water content, $w_0 = 1.7$, but with differing counterion. At this w_0 value, the ammonium−AOT surfactant has been shown to form micelles virtually identical to the regular sodium AOT.[90] By exchanging the counterion, we were able to separate the effect of the small micellar size and water interaction with other parts of the surfactant molecule from the role of the counterion. These investigations showed that the dynamics are significantly impacted by the counterion. Although the water inside the micelles is still bound by the ions, a component to the dynamics appears on the ~10 ps time scale. Therefore, the immobilization of water in the AOT reverse micelles arises largely from the interaction of the water with a high concentration of sodium ions present in the micellar interior.

Conclusions

The major results of this work reveal that interactions of water with the surfactant headgroups in AOT reverse micelles effectively eliminates bulklike solvent dynamics. This is most evident for very small reverse micelles, $w_0 < 5$. As the volume of the water pool increases in the AOT reverse micelles, more and more water molecules are free to move and reveal a dynamic relaxation on a time scale comparable to that of bulk water. However, although the solvation dynamics in the largest reverse micelles reveal a considerable fast diffusive component, the overall dynamics are still slower than observed for bulk water, suggesting that solvent motion in a reverse micellar environment is affected by the surfactant interface. Time-resolved anisotropy measurements show that the probe molecule for these measurements resides near the micellar interface.

Acknowledgment. We thank Professor Sandra J. Rosenthal for her input in building the fluorescence-upconversion spectrometer and Professor Joseph M. Beecham for a copy of the GLOBALS iterative-reconvolution program. We also thank Dr. Newton Seitzinger and Mr. Brent Coonts at Atrix Laboratories, Inc. for carrying out the Karl Fisher titration of the AOT. This work was supported by the National Science Foundation and the Petroleum Research Foundation. N.E.L. is the recipient of a National Science Foundation Young Investigator award.

References and Notes

(1) Jimenez, R.; Fleming, G. R.; Kumar, P. V.; Maroncelli, M. *Nature* **1994**, *369*, 471.

(2) Stryer, L. *Biochemistry*, 4th ed.; W. H. Freeman and Company: New York, 1995.

(3) Zuber, H. In *The Photosynthetic Reaction Center*; Deisenhofer, J., Eds.; Academic Press: San Diego, 1993; Vol. I, p 43.

(4) Menger, F. M.; Yamada, K. *J. Am. Chem. Soc.* **1979**, *101*, 6731.

(5) Corbin, D. R.; Herron, N. *J. Mol. Catal* **1994**, *86*, 343.

(6) Johnson, J. W.; Brody, J. F.; Soled, S. L.; Gates, W. E.; Robbins, J. L.; Marucchi-Soos, E. *J. Mol. Catal. A* **1996**, *107*, 67.

(7) *Structure and Reactivity in Reverse Micelles*; Pileni, M. P., Eds.; Elsevier: Amsterdam, 1989; Vol. 65.

(8) *Reverse Micelles. Biological and Technological Relevance of Amphiphilic Structures in Apolar Media*; Luisi, P. L., Straub, B. E., Eds.; Plenum Press: New York, 1987.

(9) Fendler, J. H. *J. Phys. Chem.* **1980**, *84*, 1485.

(10) Barzykin, A. V.; Tachiya, M. *Heterog. Chem. Rev.* **1996**, *3*, 105.

(11) Kalyanasundaram, K. *Photochemistry in Microheterogeneous Systems*; Academic Press: Orlando, FL, 1987.

(12) Mukherjee, L.; Mitra, N.; Bhattacharya, P. K.; Moulik, S. P. *Langmuir* **1995**, *11*, 2866.

(13) Mukhopadhyay, L.; Mitra, N.; Bhattacharya, P. K.; Moulik, S. P. *J Colloid Interface Sci* **1997**, *186*, 1.

(14) De, T.; Maitra, A. *Adv. Colloid Interface Sci.* **1995**, *59*, 95 and references therein.

(15) Frank, S. G.; Zografi, G. *J. Colloid Interface Sci.* **1968**, *28*, 66.

(16) Wong, M.; Grätzel, M.; Thomas, J. K. *Chem. Phys. Lett.* **1975**, *30*, 329.

(17) Wong, M.; Thomas, J. K.; Nowak, T. *J. Am. Chem. Soc.* **1977**, *99*, 4730.

(18) Wong, M.; Thomas, J. K.; Gratzel, M. *J. Am. Chem. Soc.* **1976**, *98*, 2391.

(19) Maitra, A. *J. Phys. Chem.* **1984**, *88*, 5122.

(20) Carnali, J.; Lindman, B.; Söderman, O.; Walderhaug, H. *Langmuir* **1986**, *2*, 51.

(21) Llor, A.; Rigny, P. *J. Am. Chem. Soc.* **1986**, *108*, 7533.

(22) Hauser, H.; Haering, G.; Pande, A.; Luisi, P. L. *J. Phys. Chem.* **1989**, *93*, 7869.

(23) Belletête, M.; Lachapelle, M.; Durocher, G. *J. Phys. Chem.* **1990**, *94*, 7642.

(24) Zhang, J.; Bright, F. V. *J. Phys. Chem.* **1991**, *95*, 7900.

(25) Jain, T. K.; Varshney, M.; Maitra, A. *J. Phys. Chem.* **1989**, *93*, 7409.

(26) Zhukovskii, A. P.; Petrov, L. N.; Rovnov, N. V. *Zh. Strukt. Khim.* **1991**, *32*, 81.

(27) Onori, G.; Ronca, M.; Santucci, A. *Prog. Colloid Polym. Sci.* **1991**, *84*, 88.

(28) Onori, G.; Santucci, A. *J. Phys. Chem.* **1993**, *97*, 5430.

(29) Amico, P.; D'Angelo, M.; Onori, G.; Santucci, A. *Nuovo Cimento* **1995**, *17*, 1053.

(30) Giammona, G.; Goffredi, F.; Liveri, V. T.; Vassallo, G. *J. Colloid Interface Sci.* **1992**, *154*, 411.

(31) Aliotta, F.; Migliardo, P.; Donato, D. I.; Turco-Liveri, V.; Bardez, E.; Larrey, B. *Prog. Colloid Polym. Sci.* **1992**, *89*, 258.

(32) Christopher, D. J.; Yarwood, J.; Belton, P. S.; Hills, B. P. *J. Colloid Interface Sci.* **1992**, *152*, 465.

(33) Moran, P. D.; Bowmaker, G. A.; Cooney, R. P. *Langmuir* **1995**, *11*, 738.

(34) Correa, N. M.; Biasutti, M. A.; Silber, J. J. *J. Colloid Interface Sci.* **1995**, *172*, 71.

(35) Cho, C. H.; Chung, M.; Lee, J.; Nguyen, T.; Singh, S.; Vedamuthu, M.; Yao, S. H.; Zhu, J. B.; Robinson, G. W. *J. Phys. Chem.* **1995**, *99*, 7806.

(36) Sarkar, N.; Das, K.; Datta, A.; Das, S.; Bhattacharyya, K. *J. Phys. Chem.* **1996**, *100*, 100523.

(37) Sarkar, N.; Datta, A.; Das, S.; Bhattacharyya, K. *J. Phys. Chem.* **1996**, *100*, 15483.

(38) Mittleman, D. M.; Nuss, M. C.; Colvin, V. L. *Chem. Phys. Lett.* **1997**, *275*, 332.

(39) Stratt, R. M.; Maroncelli, M. *J. Phys. Chem.* **1996**, *100*, 12981.

(40) Castner, E. W., Jr.; Maroncelli, M.; Fleming, G. R. *J. Chem. Phys.* **1987**, *86*, 1090.

(41) Kahlow, M. A.; Jarzeba, W.; DuBruil, T. P.; Barbara, P. F. *Rev. Sci. Instrum.* **1988**, *59*, 1098.

(42) Horng, M. L.; Gardecki, J. A.; Papazyan, A.; Maroncelli, M. *J. Phys. Chem.* **1995**, *99*, 17311.

(43) Chang, Y. J.; Castner, E. W. *J. Chem. Phys.* **1993**, *99*, 7289.

(44) Cho, M.; Rosenthal, S. J.; Scherer, N. F.; Ziegler, L. D.; Fleming, G. R. *J. Chem. Phys.* **1992**, *96*, 5033.

(45) Joo, T.; Jia, Y.; Fleming, G. R. *J. Chem. Phys.* **1996**, *104*, 6089.

(46) Yang, T. S.; Vohringer, P.; Arnett, D. C.; Scherer, N. F. *J. Chem. Phys.* **1995**, *103*, 8346.

(47) Simon, J. D. *Acc. Chem. Res.* **1988**, *21*, 128.

(48) Barbara, P. F.; Jarzeba, W. *Adv. Photochem.* **1990**, *15*, 1.

(49) Maroncelli, M. *J. Mol. Liq.* **1993**, *57*, 1.

(50) Michael, D.; Benjamin, I. *J. Phys. Chem.* **1995**, *99*, 1530.

(51) Vajda, S.; Jimenez, R.; Rosenthal, S. J.; Fidler, V.; Fleming, G. R.; Castner, E. W., Jr. *J. Chem. Soc., Faraday Trans.* **1995**, *91*, 867.

(52) Das, S.; Datta, A.; Bhattacharyya, K. *J. Phys. Chem. A* **1997**, *101*, 3299.

(53) Das, K.; Sarkar, N.; Das, S.; Datta, A.; Bhattacharyya, K. *Chem. Phys. Lett.* **1996**, *249*, 323.

(54) Awschalom, D. D.; Warnock, J. In *Molecular Dynamics in Restricted Geometries*; Klafter, J., Drake, J. M., Eds.; John Wiley & Sons: New York, 1989; p 351.

(55) Streck, C.; Melnichenko, Y. B.; Richert, R. *Phys. Rev. B: Condens. Matter* **1996**, *53*, 5341.

(56) Zulauf, M.; Eicke, H.-F. *J. Phys. Chem.* **1979**, *83*, 480.

(57) Hilfiker, R.; Eicke, H. F.; Sager, W.; Steeb, C.; Hofmeier, U.; Gehrke, R. *Ber. Bunsen-Ges. Phys. Chem.* **1990**, *94*, 677.

(58) Riter, R. E.; Kimmel, J. R.; Undiks, E. P.; Levinger, N. E. *J. Phys. Chem. B* **1997**, *101*, 8292.

(59) Keh, E.; Valeur, B. *J. Colloid Interface Sci.* **1981**, *79*, 465.

(60) Bridge, N. J.; Fletcher, P. D. I. *J. Chem. Soc., Faraday Trans.* **1983**, *79*, 2161.

(61) Pileni, M.-P.; Zemb, T.; Petit, C. *Chem. Phys. Lett.* **1985**, *118*, 414.

(62) Brucker, G. A.; Kelley, D. F. *J. Phys. Chem.* **1987**, *91*, 2856.

(63) Parsapour, F.; Kelley, D. F. *J. Phys. Chem.* **1996**, *100*, 2791.

(64) Rosenthal, S. J.; Jimenez, R.; Fleming, G. R.; Kumar, P. V.; Maroncelli, M. *J. Mol. Liq.* **1994**, *60*, 25.

(65) Siano, D. B.; Metzler, D. E. *J. Chem. Phys.* **1969**, *51*, 1856.

(66) Fee, R. S.; Maroncelli, M. *Chem. Phys.* **1994**, *183*, 235.

(67) Horng, M. L.; Gardecki, J. A.; Maroncelli, M. *J. Phys. Chem. A* **1997**, *101*, 1030.

(68) Krishnakumar, S.; Somasundaran, P. *J. Colloid Interface Sci.* **1994**, *162*, 425.

(69) Jarzeba, W.; Walker, G. C.; Johnson, A. E.; Kahlow, M. A.; Barbara, P. F. *J. Phys. Chem.* **1988**, *92*, 7039.

(70) Zolotov, B.; Gan, A.; Fainberg, B. D.; Huppert, D. *Chem. Phys. Lett.* **1997**, *265*, 418.

(71) Nandi, N.; Roy, S.; Bagchi, B. *J. Chem. Phys.* **1995**, *102*, 1390.

(72) Chapman, C. F.; Maroncelli, M. *J. Phys. Chem.* **1991**, *95*, 9095.

(73) Bart, E.; Huppert, D. *Chem. Phys. Lett.* **1992**, *195*, 37.

(74) Huppert, D.; Ittah, V.; Kosower, E. M. *Chem. Phys. Lett.* **1989**, *159*, 267.

(75) Ittah, V.; Huppert, D. *Chem. Phys. Lett.* **1990**, *173*, 496.

(76) Chandra, A.; Patey, G. N. *J. Chem. Phys.* **1994**, *100*, 1552.

(77) Chandra, A. *Chem. Phys. Lett.* **1995**, *244*, 314.

(78) Neria, E.; Nitzan, A. *AIP Conf. Proc.* **1994**, *298*, 368.

(79) Neria, E.; Nitzan, A. *J. Chem. Phys.* **1994**, *100*, 3855.

(80) Guàrdia, E.; Padró, J. A. *J. Phys. Chem.* **1990**, *94*, 6049.

(81) Impey, R. W.; Madden, P. A.; McDonald, I. R. *J. Phys. Chem.* **1983**, *87*, 5071.

(82) Jiang, Y.; Mccarthy, P. K.; Blanchard, G. J. *Chem. Phys.* **1994**, *183*, 249.

(83) Willard, D. M.; Riter, R. E.; Levinger, N. E. *J. Am. Chem. Soc.*, in press.

(84) Kahlow, M. A.; Kang, T. J.; Barbara, P. F. *J. Chem. Phys.* **1988**, *88*, 2372.

(85) Nagarajan, V.; Brearley, A. M.; Kang, T.-J.; Barbara, P. F. *J. Chem. Phys.* **1987**, *86*, 3183.

(86) Nandi, N.; Bagchi, B. *J. Phys. Chem.* **1996**, *100*, 13914.

(87) Brown, D.; Clarke, J. H. R. *J. Phys. Chem.* **1988**, *92*, 2881.

(88) Linse, P. *J. Chem. Phys.* **1989**, *90*, 4992.

(89) Riter, R. E.; Undiks, E. P.; Levinger, N. E. *J. Am. Chem. Soc.*, submitted.

(90) Eastoe, J.; Robinson, B. H.; Heenan, R. K. *Langmuir* **1993**, *9*, 2820.

(91) We have performed a Student *t* test on our data to make a quantitative comparison with data reported in the literature and find that our results lie within one standard deviation of all the published data (Jimenez et al.,[1] Vajda et al.,[51] and Jarzeba et al.[69]).